Electronic Supplementary Information for

A hierarchical heterostructure based on Pd nanoparticles/layered double hydroxide nanowalls for enhanced ethanol electrooxidation

Jingwen Zhao,[a] Mingfei Shao,[a] Dongpeng Yan,[a] Shitong Zhang,[a] Zhenzhi Lu,[a] Zhuoxin Li,[b] Xingzhong Cao,[b] Baoyi Wang,[b] Min Wei,*[a] David G. Evans[a] and Xue Duan[a]

[a] *State Key Laboratory of Chemical Resource Engineering, Beijing University of Chemical Technology, Beijing 100029, China*

[b] *Institute of High Energy Physics, Chinese Academy of Sciences, Beijing 100049, China*

CORRESPONDING AUTHOR FOOTNOTE

* Corresponding author. Tel: +86-10-64412131; Fax: +86-10-64425385.

E-mail address: weimin@mail.buct.edu.cn (Min Wei).

Computational details

All calculations were performed with the periodic density functional theory (DFT) method using Dmol3 module in Material Studio 5.5 software package (Accelrys Inc.: San, Diego, CA).[1] A Pd_9 cluster model was used to represent the local structure of the Pd(111) surface which dominates the structure of the Pd-based electrocatalyst. The palladium metal lattice belongs to the face centered cubic structure. An ideal LDH layer containing 12 Co atoms and 6 Al atoms was built on the basis of each [AlO_6] octahedron surrounded by six [CoO_6] octahedra and each [CoO_6] octahedron, in turn, surrounded by three [AlO_6] octahedra, owing to the molar ratio of Co/Al=2:1, which ensures that Al atoms will not occupy adjacent octahedra.[2] In this case, every octahedral layer has 18 metal atoms and 36 OH groups, and a supercell was constructed with lattice parameters $a = 18.41$ Å, $b = 9.20$ Å, $\alpha = \beta = 90°$, $\gamma = 120°$ (equivalent to 6 × 3 × 1 in the *a*, *b*, *c* directions), which is in accordance with the literature.[3] A surface model was cleaved from this supercell to simulate the (001) surface of the CoAl-LDH, which contains a host layer and three

CO_3^{2-}. The neighboring slabs are separated in the direction perpendicular to the surface by a vacuum distance of 12 Å. The generalized gradient approximation (GGA) with the Perdew−Burke−Ernzerhof (PBE)[4] functional, and effective core potentials with double-numeric quality basis were utilized for the geometric optimization and single-point energy calculations. During the calculations, the convergence tolerance was set as follows: energy = 1.0×10^{-6} Ha, force = 1.0×10^{-3} Ha/Å, displacement = 1.0×10^{-3} Å.

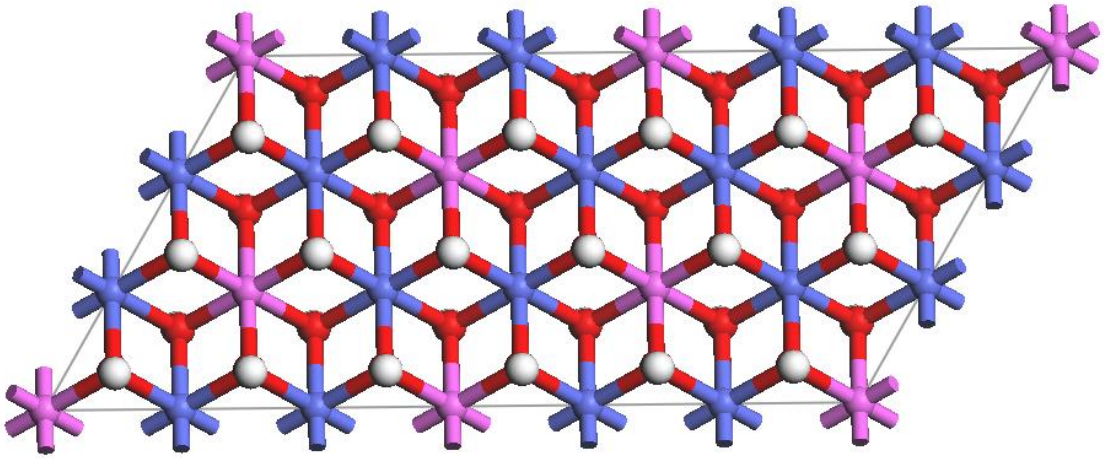

Scheme S1. The supercell model for CoAl-LDH layer with 6 × 3 × 1 rhombohedral lattice (color codes: white, H; pink, Al; red, O; blue, Co).

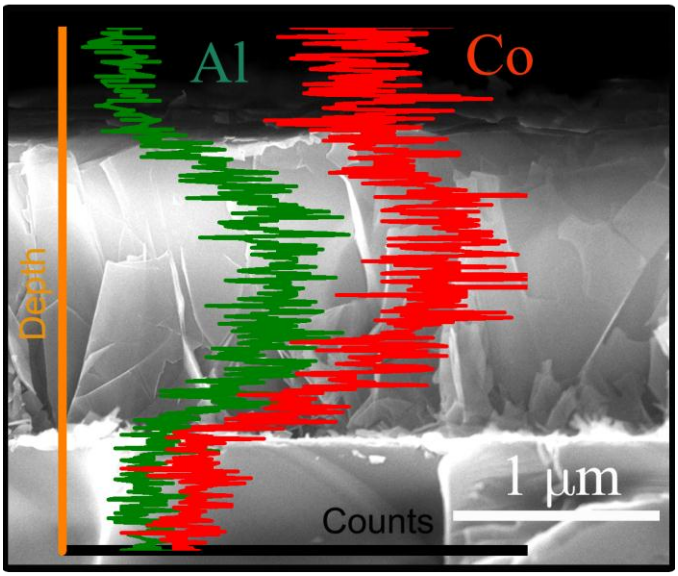

Fig. S1. Cross-sectional SEM image of the LDH-NWs with the corresponding EDS line scan.

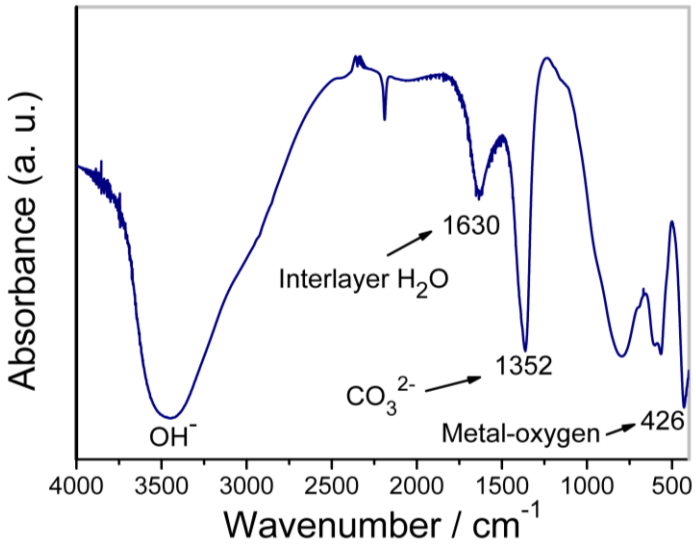

Fig. S2. FT-IR spectrum of the LDH-NWs.

The FT-IR spectrum (Fig. S2) provides evidence for the presence of carbonate (CO_3^{2-}) existing in the LDH gallery (band at ~1352 cm^{-1}); the characteristic bands of metal-oxygen in the brucite-like lattice are observed below 800 cm^{-1}, especially the strong band at ~426 cm^{-1}.[5]

Heterogeneous nucleation on a substrate can be promoted at a lower supersaturation of reagents over homogeneous nucleation in solution due to the absence (or at least trace amount) of precipitate in solution. The supersaturation of reagents can be controlled by, for example, using complexing agents to release metal ions gradually. In this work, with the assistance of NH_4F, coordinated CoF_x and AlF_x formed in the as-prepared homogeneous solution firstly; Co^{2+} and Al^{3+} ions were released slowly into the reaction system for the formation of CoAl nuclei on the substrate.

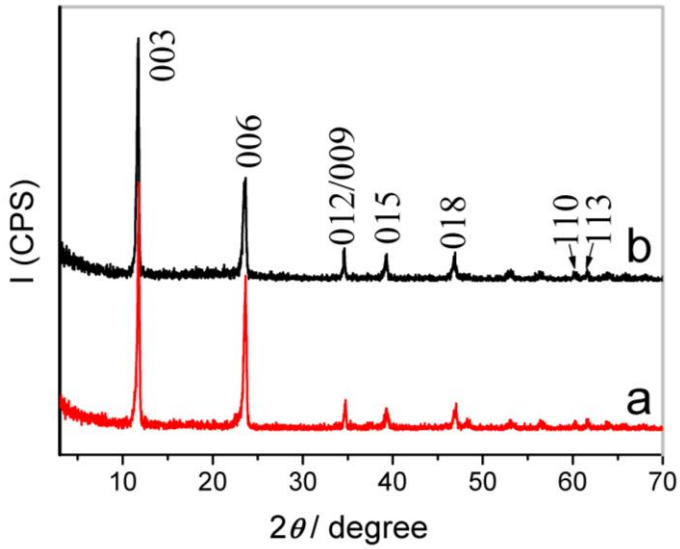

Fig. S3. XRD patterns of (a) CoAl-LDH and (b) PdNPs/CoAl-LDH powdered samples.

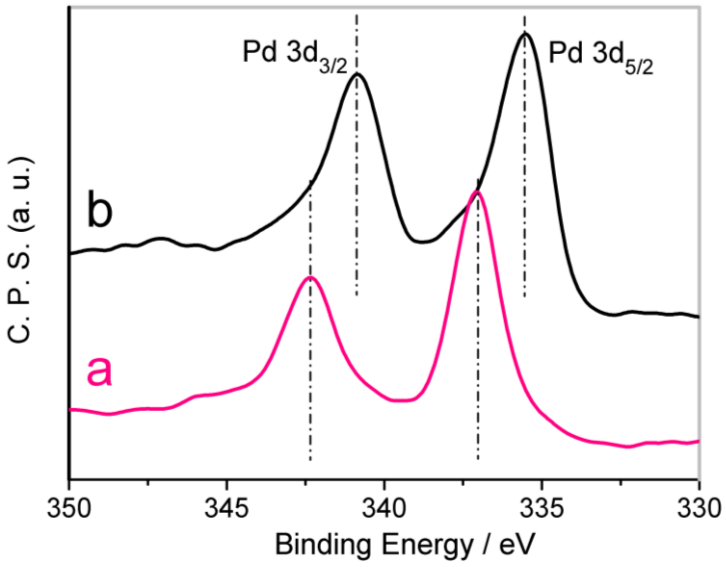

Fig. S4. XPS spectra of Pd 3d in (a) MgAl-LDH and (b) CoAl-LDH after immersing in a $PdCl_4^{2-}$ aqueous solution for 20 min at the room temperature.

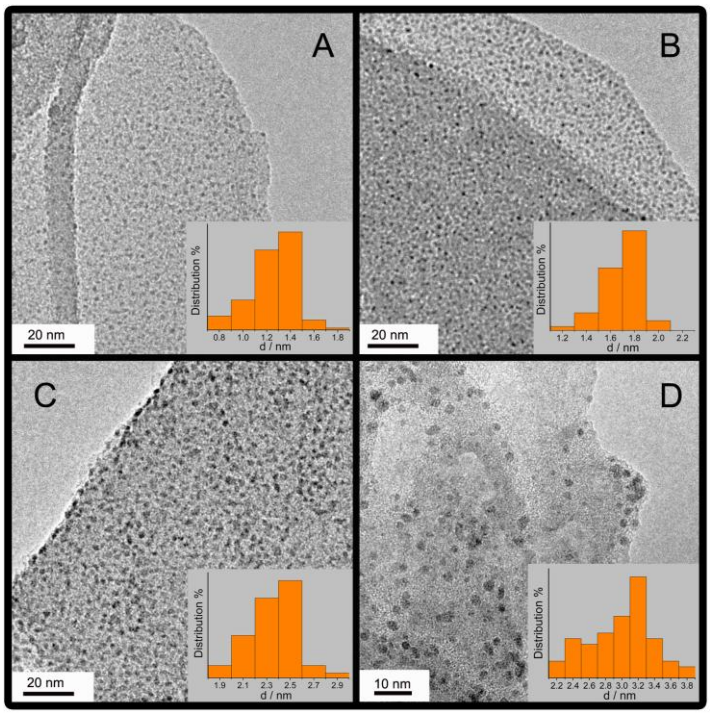

Fig. S5. TEM images and corresponding size distribution histogram of PdNPs on the LDH-NWs substrate with various deposition temperatures: (A) 0 °C, (B) 25 °C, (C) 50 °C, and (D) 80 °C.

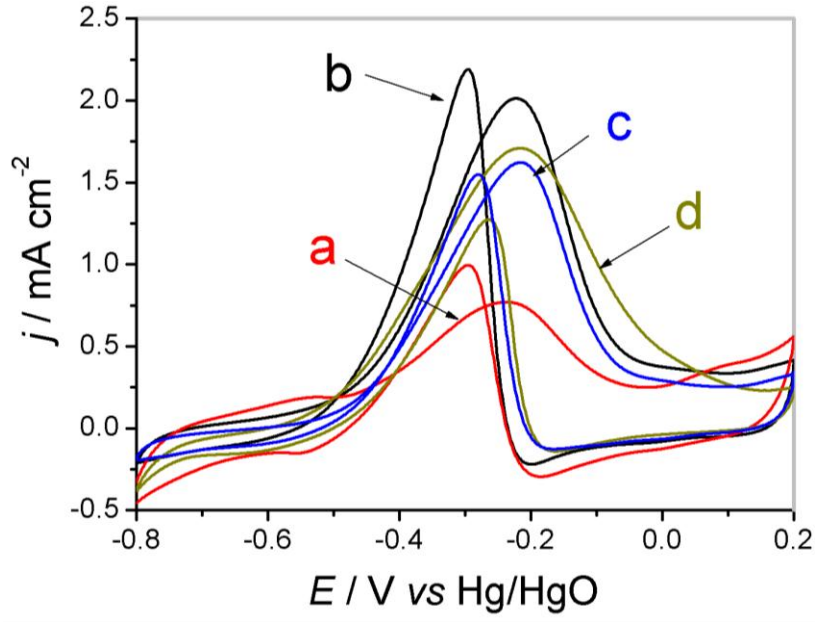

Fig. S6. Cyclic voltammograms of Pd/LDH-NWs synthesized at (a) 0 °C, (b) 25 °C, (c) 50 °C, (d) 80 °C for ethanol electrooxidation at 50 mV s^{-1}.

The particle size can be readily tuned by changing the temperature of PdNPs deposition. Increasing the reaction temperature in the range 0−80 °C results in the obvious growth of PdNPs (Fig. S4). However, as the reaction temperature is over 50 °C, a significant increase in the particle size and a decrease in the PdNPs density are observed, which is ascribed to the well-known Ostwald ripening occurring at high temperature. The resulting electrocatalytic activity of these samples is depicted in Fig. S5, from which the oxidation current shows a gradual enhancement as the temperature increases from 0 to 25 °C; while a decrease in peak current and a positive shift in potential are observed with further increasing the temperature. The results indicate that the PdNPs obtained at 25 °C (particle size: ~1.8 nm) possess the highest activity owing to the high-density and high-dispersion of metal particles (shown in Fig. S4B); whereas the decreased catalytic activity for the sample with higher deposition temperature is associated with the weakening in anchoring ability of PdNPs onto the LDH surface due to the Ostwald ripening process.

Table S1. Peak current densities of ethanol electrooxidation on the Pd/LDH-NWs for different potential cycles

Current	j_F/mA cm^{-2}	j_F/ $j_{F(1st)}$	j_R/mA cm^{-2}	j_R/ $j_{R(1st)}$
1st	2.01	/	2.19	/
200th	2.00	99.5%	1.99	90.8%
500th	1.93	96.0%	1.92	87.6%

Table S2. Peak current densities of ethanol electrooxidation on various electrodes after 500 potential cycles

Current	$j_{F(1st)}$/ mA cm^{-2}	$j_{F(500th)}$/ mA cm^{-2}	$j_{F(500th)}$/ $j_{F(1st)}$	$j_{R(1st)}$/ mA cm^{-2}	$j_{R(500th)}$/ mA cm^{-2}	$j_{R(500th)}$/ $j_{R(1st)}$
Pd/LDH-NWs	2.01	1.93	96.0%	2.19	1.92	87.6%
Pd/C	0.41	0.28	68.3%	0.35	0.20	57.1%
Pd/LDH	0.52	0.43	82.6%	0.55	0.42	76.3%

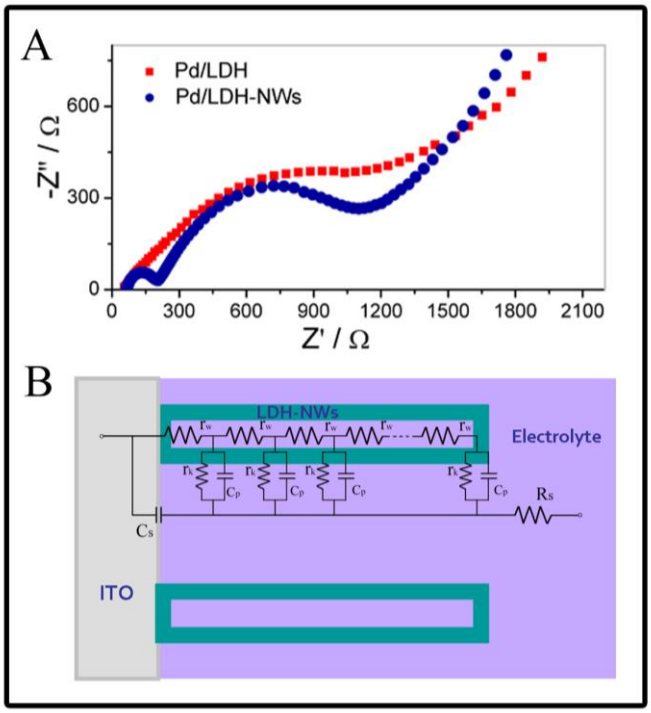

Fig. S7. (A) Nyquist plots of the impedance data for the Pd/LDH-NWs and Pd/LDH with $Fe[(CN)_6]^{4-/3-}$ as the redox probe. (B) Equivalent circuit model of the Pd/LDH-NWs electrode.

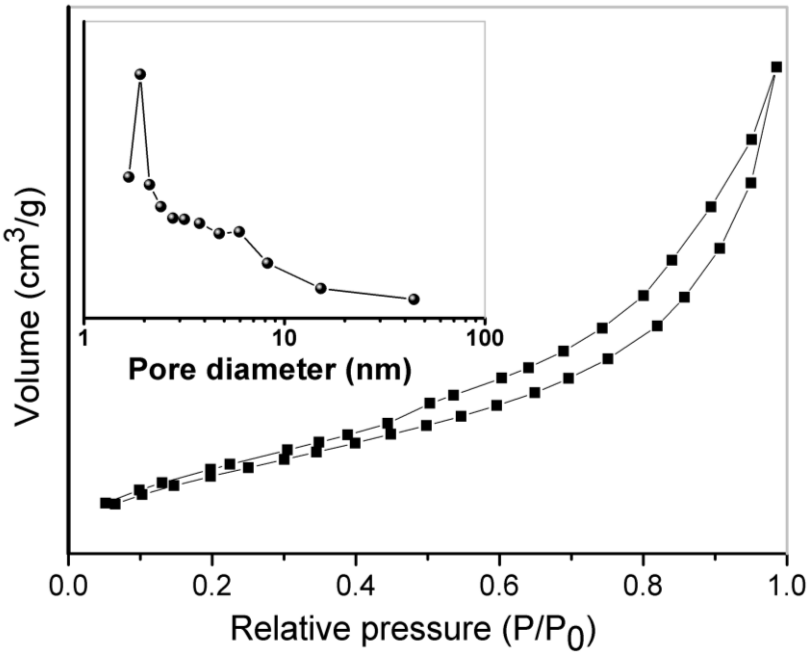

Fig. S8. Nitrogen adsorption-desorption isotherms and corresponding pore size distribution (inset) for the Pd/LDH-NWs.

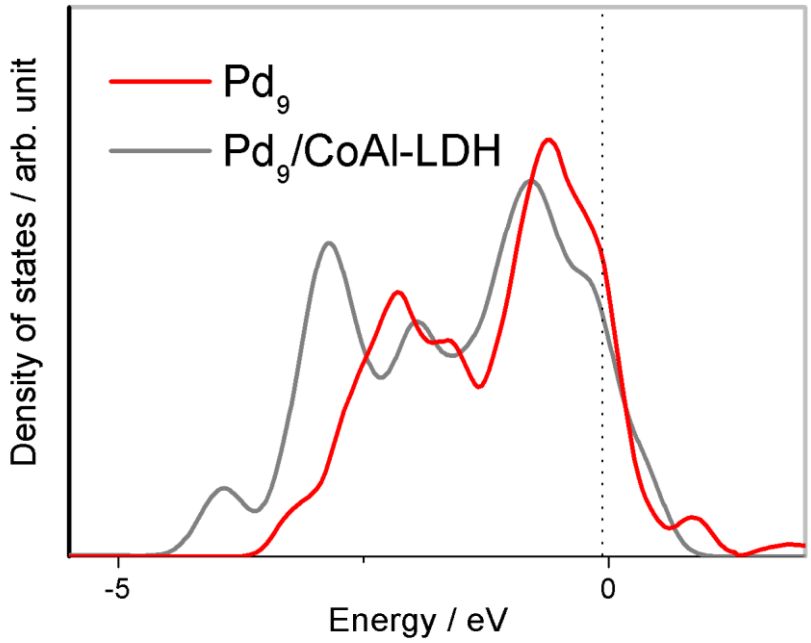

Fig. S9. Local density of states (LDOS) of Pd_9 (Pd d state): pristine Pd_9 (red) and Pd_9/CoAl-LDH system (grey). The Fermi level (black dashed line) as the reference of zero energy.

Table S3. Positron lifetime of the three samples

Sample	τ_1 (ps)	I_1 (%)	τ_2 (ps)	I_2 (%)	τ_3 (ps)	I_3 (%)
CoAl-LDH	208.0	26.30	331.9	71.70	2.211	2.02
Pd/CoAl-LDH	200.0	30.50	333.7	67.90	2.324	1.60
Pd	109.5	100.0	—	—	—	—

Positron annihilation technique was employed for investigating electronic environment of the CoAl-LDH, Pd/CoAl-LDH and pristine Pd (Table S3). The positron lifetime spectra were resolved into three components (τ_1 , τ_2 and τ_3) with relative intensities (I_1 , I_2 , and I_3). The longest component in excess of ~1 ns (τ_3) is generally indicative of the annihilation of ortho-positronium (*o*-Ps) formed in the pores or large voids present in the material. It should be mentioned that the *o*-Ps could be annihilated faster by electrons from the surrounding medium through the pickoff process.[6] For the LDH materials, τ_3 mainly originates from the annihilation of the sub-nanometre free volume holes present in the interlayer spacings.[7] Loading of PdNPs onto the LDH surface

leads to a rise of τ_3, indicating the reduction in electron density in the LDH phase in line with the redox process between LDH and $PdCl_4^{2-}$. Furthermore, an inhibition effect on the *o*-Ps formation was observed for the sample of Pd/CoAl-LDH, which is evidenced by the decrease of I_3 from 2.02% to 1.60%. The shortest component (τ_1) is associated with para-positronium (*p*-Ps) annihilation and positron annihilation in the free state (also named as the bulk positron lifetime).[8] Owing to the higher average electron density, the pristine Pd possesses a smaller value of τ_1 (109.5 ps) than the CoAl-LDH (208.0 ps). After immobilization of PdNPs, τ_1 slightly decreases from 208.0 ps (CoAl-LDH) to 200.0 ns (Pd/CoAl-LDH), and the intensity I_1 increases from 26.3% to 30.5%, suggesting the prior trapping and annihilation of positrons near the PdNPs with enhanced electron density.

References:

1 (a) M. D. Segall, P. J. D. Lindan, M. J. Probert, J. Pickard, P. J. Hasnip, S. J. Clark and M. C. Payne, *J. Phys. Condens. Matter*, 2002, **14**, 2717; (b) B. Delley, *J. Chem. Phys.*, 1990, **92**, 508.

2 P. J. Sideris, U. G. Nielsen, Z. Gan and C. P. Grey, *Science*, 2008, **321**, 113.

3 R. E. Johnsen, F. Krumeich and P. Norby, *J. Appl. Cryst.*, 2010, **43**, 434.

4 (a) J. P. Perdew, K. Bruke and M. Ernzerhof, *Phys. Rev. Lett.*, 1996, **77**, 3865; (b) G. Kresse and J. Joubert, *Phys. Rev. B*, 1999, **59**, 1758.

5 J. Han, Y. Dou, M. Wei, D. G. Evans and X. Duan, *Angew. Chem. Int. Ed.*, 2010, **49**, 2171.

6 S. Chakraverty, S. Mitra, K. Manda, P. M. G. Nambissan and S. Chattopadhyay, *Phys. Res. B*, 2005, **71**, 024116.

7 N. Fong, P. Guagliardo, J. Williams, A. Musumeci, D. Martin and S. V. Smith, *J. Phys.: Conf. Ser.*, 2011, **262**, 012022.

8 (a) M. Mukherjee, D. Chakravorty and P. M. G. Nambissan, *Phys. Res. B*, 1998, **57**, 848; (b) S. Dannefaer, T. Bretagnon and D. Kerr, *J. Appl. Phys.*, 1993, **74**, 884.